Multiple Sclerosis and Related Disorders 41 (2020) 102008

Contents lists available at ScienceDirect

Multiple Sclerosis and Related Disorders

journal homepage: www.elsevier.com/locate/msard

Original article

Which is the best PML risk stratification strategy in natalizumab-treated patients affected by multiple sclerosis?

Carla Prezioso[a,b], Maria Antonella Zingaropoli[a], Marco Iannetta[c], Donatella Maria Rodio[a], Marta Altieri[d], Antonella Conte[d,e], Vincenzo Vullo[a], Maria Rosa Ciardi[a], Anna Teresa Palamara[b,f], Valeria Pietropaolo[a,*]

[a] Department of Public Health and Infectious Diseases, "Sapienza" University, P.le Aldo Moro, 5, 00185 Rome, Italy
[b] IRCSS San Raffaele Pisana, Microbiology of Chronic Neuro-degenerative Pathologies, Rome, Italy
[c] Department of System Medicine Infectious Disease Clinic, Tor Vergata University, Rome, Italy
[d] Department of Human Neurosciences, Sapienza University, Rome, Italy
[e] IRCCS Neuromed, Pozzilli, IS, Italy
[f] Department of Public Health and Infectious Diseases, Institute Pasteur, Cenci-Bolognetti Foundation, Sapienza University of Rome, Italy

ARTICLE INFO

Keywords:
Biomarkers
Natalizumab
Anti-JCPyV-antibodies
JCPyV DNA-detection
NCCR arrangements

ABSTRACT

Background: The risk of progressive multifocal leukoencephalopathy (PML), a brain infection caused by John Cunningham virus (JCPyV), is the main limitation to the use of natalizumab, highly effective in the treatment of relapsing remitting multiple sclerosis (RRMS) patients. Establishing the PML risk against expected benefits represents an obligatory requirement of MS treatment algorithm. In order to achieve this goal, the aims of this study were to establish if JCPyV-DNA detection and non-coding control region (NCCR) arrangements could play a role of *biomarkers,* supporting anti-JCPyV antibodies measurement, actually the only parameter for PML risk stratification.

Methods: Thirty RRMS patients in treatment with natalizumab were enrolled. Urine and blood samples were collected according to this calendar: baseline (T0), 4 (T1), 8 (T2), 12 (T3), 16 (T4), 20 months (T5) after beginning of natalizumab therapy. After JCPyV DNA extraction, a specific quantitative-PCR (Q-PCR) and arrangements' analysis of NCCR and Viral Capsid Protein 1 (VP1) were carried out.

Results: Q-PCR detected JCPyV DNA in urine and blood from baseline (T0) to 20 natalizumab infusions (T5), although JC viral load in urine was significantly higher compared to viremia, at all selected time points. A contextual analysis of the anti-JCPyV-antibodies versus JCPyV-DNA detection revealed that viral DNA preceded the antibodies' presence in the serum. During the first year of natalizumab treatment, sequences isolated from blood displayed an archetype JCPyV NCCR structure with the occurrence of point mutations, whereas after one year NCCR re-organizations were observed in plasma and PBMC with duplication of NF-1 binding site in box F, duplication of box C and partial or total deletion of box D. VP1 analysis showed the amino acid change mutation S269F in plasma and S267L in PBMC, involving the receptor-binding region of VP1. Phylogenetic analysis suggested a stability and a similarity across different isolates of the JCPyV VP1.

Conclusions: We highly recommend considering JCPyV-DNA detection and NCCR re-organizations as viral *biomarkers* in order to accurately identify JCPyV-infected patients with a specific humoral response not yet detectable and to identify NCCR arrangements correlated with the onset of neurovirulent variants.

1. Introduction

The arsenal of medications for the treatment of multiple sclerosis (MS), a complex chronic, autoimmune, demyelinating disease affecting central nervous system (CNS) (Browne et al., 2014), has been enriched by a variety of substances with differing mechanisms of action. Specifically, to date, 13 disease-modifying therapies (DMTs) for treatment of relapsing-remitting multiple sclerosis (RRMS), the most prevalent MS phenotype, have been approved by the Food and Drug Administration (FDA) and have changed the scenery for care of RRMS patients (Tintore et al., 2019). Although these newer drugs allowed long periods of disease activity-free remission (Giovannoni et al., 2018),

* Corresponding author.
E-mail address: valeria.pietropaolo@uniroma1.it (V. Pietropaolo).

https://doi.org/10.1016/j.msard.2020.102008
Received 2 December 2019; Received in revised form 3 February 2020; Accepted 10 February 2020

they are also correlated with a higher risk of serious side effects. Several DMTs have been associated with progressive multifocal leukoencephalopathy (PML), a demyelinating disease of CNS, caused by John Cunningham virus (JCPyV) (Pietropaolo et al., 2018). PML evolves in the context of an underlying immunological anomaly and in cell-mediated immunity deficiency, as demonstrated by more than 60% of PML cases occurred in association with hematological malignancies (Brooks and Walker, 1984) or during AIDS pandemic (Berger et al., 1987). In 2005, two individuals with MS (Kleinschmidt-DeMasters and Tyler, 2005) and one with Crohn's disease (Van Assche et al., 2005) developed PML after natalizumab treatment. Natalizumab (Tysabri®), Biogen. TYSABRI® (natalizumab) 2016 the most potent effective DMT for relapse prevention, is a monoclonal antibody which prevents the linkage between α4β1 and its ligand (vascular cell adhesion molecule-1) blocking transmigration of activated lymphocytes into CNS (Clerico et al., 2017). This blocking attenuates the CNS inflammation, however, promotes a decrease in immune-surveillance and JCPyV re-activation from latency (Berger, 2017).

JCPyV is a neurotropic virus isolated from the brain of a patient who died with PML (Padgett et al., 1971). Early and late coding regions of JCPyV genome are highly conserved (Ciotti et al., 2019). Dissimilarity, non-coding control region (NCCR) is highly variable and characterized by determinants of neurovirulence (Pietropaolo et al., 2018). Archetype NCCR, divided into six boxes from A to F, (Yogo et al., 1990), undergoing deletion and enhancement processes, could generate arranged NCCR (*rr*-NCCR) sequences, observed during host's immunosuppression and correlated with a poor prognosis in PML patients.

In the last two decades, several studies have been carried out in order to identify markers which could improve safety and efficacy of natalizumab therapy, nevertheless PML cases were reported (Major et al., 2018). As of May 2016, the global incidence of PML during natalizumab treatment was 4.22 per 1000 patients. (https://medinfo.biogen.com/). Three factors stratify risk: natalizumab therapy > 2 years, an antibodies index for JCPyV > 1,5 and previous immunosuppressive therapy (Wingerchuk and Weinshenker, 2016). Actually, anti-JCPyV antibodies index is the only parameter for PML risk stratification, although many others candidates, such as L-selectin (CD62L) expression, T-cell response to JCPyV reactivation in PML, microRNAs expression during natalizumab therapy (Wingerchuk and Weinshenker, 2016) and JCPyV-DNA detection in blood (viremia) have been proposed (Mancuso et al., 2012; Pietropaolo et al., 2015). Since the risk of PML is the main limitation to natalizumab administration, highly effective in reducing annualized relapse rate (ARR) of 55% (Polman et al., 2006), establishing risk against expected benefits represents an obligatory requirement of MS treatment algorithm. In order to achieve this goal, this study was conducted on a RRMS *cohort* of patients in treatment with natalizumab to establish if JCPyV-DNA detection in different body compartments and NCCR arrangements could play a role of *biomarkers,* supporting anti-JCPyV antibodies measurement and contributing to PML risk monitoring and assessment in the individual-patient during therapy. Moreover, to further understand if natalizumab might affect JCPyV strains circulating in our *cohort*, a Viral Capsid Protein 1 (VP1) alignment and a phylogenetic analysis were performed.

2. Methods

2.1. Study participants and samples collection

After signed informed consent based on the approved Ethic Committee of Policlinico Umberto I of Rome (protocol number 130/13), a *cohort* of 30 RRMS subjects, followed up at the Department of Human Neurosciences of Sapienza University of Rome, was recruited between March 2016 and March 2018. All participants fulfilled the Italian Agency of Drug (AIFA) criteria for natalizumab treatment. Therapeutic protocol consisted of administration of 300 mg intravenous natalizumab every 4 weeks. The enrolled patients (12 males/18 females, mean age ± stand. dev. 30.2 ± 6.6; mean months of illness ± stand. dev. 85 ± 85.5; mean Expanded Disability Status Scale (EDSS) ± stand. dev. 1.9 ± 1.3) were visited before natalizumab treatment (baseline: 0 infusions) and every 4, 8, 12, 16, 20 infusions. Demographic and clinical characteristics are presented in Table 1.

Table 1
RRMS patients' demographic and clinical characteristics.

Variables	RRMS (n = 30)
Age years (mean, SD)	30.2 ± 6.6
Sex, female (n) and male (n)	female (18) and male (12)
Mean months of illness years (SD)	85 ± 85.5
Mean EDSS (SD)	1.9 ± 1.3
Therapy before starting natalizumab	
No therapy (/n)	12/30
Interferon β (/n)	15/30
Mitoxantrone and interferon β (/n)	2/30
Glatiramer acetate (/n)	1/30

RRMS: Relapsing-remitting multiple sclerosis; N: Number; SD: Standard deviation; EDSS: Expanded disability status scale.

Samples were collected according to this calendar: baseline (T0), 4 (T1), 8 (T2), 12 (T3), 16 (T4), 20 months (T5) after beginning of therapy. In detail, 30 plasma and 30 peripheral blood mononuclear cells (PBMC) (from whole blood in EDTA) and 30 urine samples were obtained for a total of 540 specimens.

After the activation of the STRATIFY JCV® service (Biogen Idec), assessment of anti-JCPyV antibodies (IgG) on serum of the enrolled subjects was performed at T0 and after 1 year from the start of the follow-up (T3) (Gorelik et al., 2010). At each follow-up visit, disease activity has been assessed by EDSS, with values ranging from 0 (normal neurological examination) to 10 (death due to MS) (Kurtzke, 1983). Magnetic resonance imaging (MRI) was performed at the beginning of therapy and eventually during treatment. Finally, a lumbar puncture was performed in case of neuro–radiological or clinical alterations, concomitant to JCPyV replication in blood.

2.2. Virological investigations

JCPyV DNA was extracted using DNeasy Blood & Tissue Kit (QIAGEN, Italy). Extraction products were analyzed by a quantitative PCR (Q-PCR) system able to detect and quantify a 54 bp amplicon in JCPyV T antigen region, using a 7300 real-time PCR system (Applied Biosystems) and following published protocol (Delbue et al., 2008). Each sample was analyzed in triplicate, and JCPyV DNA loads (given as the mean of at least three positive reactions) were expressed as genome equivalents (gEq)/milliliter for plasma and urine and as genome equivalents (gEq)/10^6 cells for PBMC. Negative and positive controls were included in each Q-PCR session. Standard curve was obtained from serial dilutions (range: 10^5–10^2 gEq/mL) of a plasmid containing the entire JCPyV genome. The lower detection limit of the Q-PCR system was 10 DNA copies of the target gene per amplification reaction, corresponding to 10 genome equivalents per reaction (10 gEq/reaction). JCPyV DNA positive samples were further analyzed using nested-PCR for NCCR and VP1 regions' amplification (Flaegstad et al., 1991; Markowitz et al., 1993; Jin et al., 1993). PCR products were analyzed on 2% agarose gels. The amplified products were purified using MinElute PCR Purification Kit (QIAGEN, Italy) and sequenced in a dedicated facility (Bio-Fab research, Italy). Obtained sequences were compared to reference strain (GenBank: AB081613). Sequence alignment was obtained using ClustalW2 (http://www.ebi.ac.uk/Tools/msa/clustalw2/) on the European Molecular Biology Laboratory–European Bioinformatics Institute (EMBL–EBI) website using default parameters. JCPyV genotypes/subtypes were classified based on single

nucleotide polymorphisms (SNPs) found within the amplified VP1 region (Jobes et al., 2001).

2.3. VP1 phylogenetic analysis

In phylogenetic analysis, representative strains obtained from urine, plasma and PBMC were compared with JCPyV reference (AB081613) and aligned using ClustalW2. Phylogenetic tree was created using Molecular Evolutionary Genetics Analysis (Mega), using neighbor joining algorithm (Kumar et al., 2008). A bootstrap test with 1000 replicates was performed to evaluate the confidence of the branching pattern of the trees.

2.4. Statistical analysis

JCPyV detection was summarized by counts and proportions. If continuous variables were normally distributed, they were expressed as mean ± SD; if not, they were expressed by median and range. The χ^2 test was performed to evaluate differences in the viral detection and the Mann–Whitney *U test* for non-normally distributed continuous variables was applied to analyze differences between patients. A p value < 0.05 was considered statistically significant.

3. Results

3.1. Trend of JC viral load

At baseline (T0), JCPyV DNA was found in 10 out of 30 RRMS patients enrolled. Specifically, viral DNA was found in urine (viruria) of 4 patients with an average value of 3×10^4 gEq/mL and in 3 patients' plasma (viremia), with an average value of 3.5×10^3 gEq/mL. In 2 patients, JCPyV DNA was found in PBMC with an average value of 8×10^2 gEq/10^6 cells. In one patient viral DNA was detected in plasma (1×10^3 gEq/mL) and in PBMC (4.5×10^2 gEq/10^6 cells), simultaneously (Fig. 1, Table 2). At T1 (4 natalizumab infusions), 15 RRMS patients presented JCPyV DNA: 9 had viruria (average value: 7.5×10^4 gEq/mL), 3 exhibited viremia (average value: 4×10^3 gEq/mL), whereas 2 patients showed a JCPyV DNA positivity in PBMC (average value: 1×10^3 gEq/10^6 cells). The only patient positive to JCPyV DNA both in plasma and PBMC at T0, was found positive at T1 yet (plasma: 9.5×10^2 gEq/mL; PBMC: 3×10^2 gEq/10^6 cells) (Fig. 1, Table 2). After 8 natalizumab infusions (T2), 23/30 patients presented JCPyV DNA: 15 in urine (average value: 9.5×10^4 gEq/mL), 4 were viremic (average value: 6.5×10^3 gEq/mL), 3 were positive in PBMC (average value: 1×10^3 gEq/10^6 cells). The simultaneous presence of JCPyV DNA found at T0 and T1 in one patient, was maintained, although with an increase in plasma (9×10^2 gEq/mL) and PBMC (3.5×10^2 gEq/10^6 cells) viral loads (Fig. 1, Table 2).

At T3 (12 natalizumab infusions), all RRMS patients revealed JCPyV DNA: 18 exhibited viruria (average value: 2.5×10^5 gEq/mL), 7 viremia (average value: 7×10^3 gEq/mL), 5 were positive in PBMC (average value: 1.5×10^3 gEq/10^6 cells), whereas the patient, previously positive in plasma and PBMC simultaneously, confirmed the infection only in plasma (Fig. 1, Table 2).

Results obtained after 16 natalizumab infusions (T4) showed that 22/30 patients displayed viruria (average value: $5{,}5 \times 10^5$ gEq/mL), 6 viremia (average value: 4×10^4 gEq/mL) and 5 were JCPyV DNA positive in PBMC (average value: 3×10^3 gEq/10^6 cells). The patient positive only in plasma at T3, became positive in both plasma and PBMC with an average value of $3{,}5 \times 10^4$ gEq/mL and 1×10^2 gEq/10^6 cells, respectively. Moreover, 6 patients were positive both in urine (average value: $2{,}5 \times 10^5$ gEq/mL) and plasma (average value: 3×10^4 gEq/mL) samples (Fig. 1, Table 2).

At T5 (20 natalizumab infusions), excretion of JCPyV DNA in urine occurred in 25 patients (average value: $9{,}5 \times 10^5$ gEq/mL). Nine patients presented viremia (average value: $5{,}5 \times 10^4$ gEq/mL), whereas 5 showed a JCPyV DNA in PBMC (average value: 4×10^3 gEq/10^6 cells). The patient positive to JCPyV DNA in plasma and PBMC at T0, T1, T2 and T4, showed, once again, JCPyV DNA only in plasma. The same six patients already positive in urine and plasma at T4, confirmed JCPyV DNA at T5 (urine average value: $6{,}5 \times 10^5$ gEq/mL; plasma average value: $3{,}5 \times 10^4$ gEq/mL) (Fig. 1, Table 2).

Statistical analysis of Q-PCR results indicated that the average value of JCPyV viral load detected in urine samples was significantly higher than that observed in plasma and in PBMCs ($p \leq 0.05$) (Fig. 2).

3.2. Contextual analysis of the anti-JCPyV antibodies versus JCPyV-DNA detection

Before starting natalizumab treatment (T0) and after 12 natalizumab infusion (T3), a second-generation assay (STRATIFY JCV® DxSelect™), was performed on serum of the 30 RRMS subjects. At T0, JCPyV-specific antibodies were observed in serum of 8 patients (STRATIFY JCV®-positive), whereas 22 showed a negative STRATIFY JCV® (Table 3). Contextually to the analysis of the anti-JCPyV antibodies, 10/30 patients revealed a JCPyV-DNA positivity: 1 among 8 STRATIFY

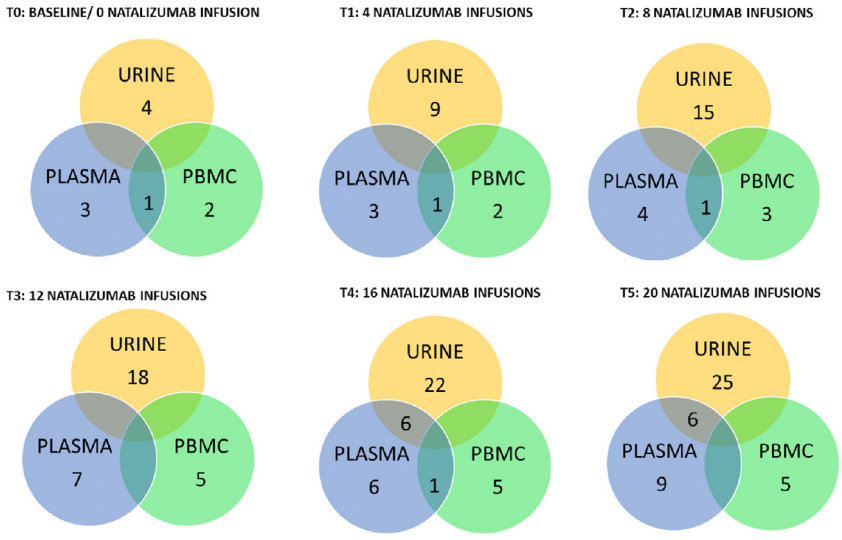

Fig. 1. Venn diagram showing the number of patients positive to JCPyV DNA in urine (viruria), plasma (viremia) and in PBMC at different time of natalizumab infusions. The number of patients presenting JCPyV DNA in multiple samples simultaneously (plasma and PBMC, urine and plasma) (shadow zone) is also reported.

Table 2
Average value of JC viral load detection in urine, plasma and PBMC during the whole study.

SAMPLE TYPE	*n*° + PATIENTS	T0: baseline JCPyV average value	T0: baseline JCPyV average value
Urine	4	3×10^4 gEq/mL	
Plasma	3	$3{,}5 \times 10^3$ gEq/mL	
PBMC	2	8×10^2 gEq/10^6 cells	
Plasma + PBMC	1	1×10^3 gEq/mL	$4{,}5 \times 10^2$ gEq/10^6 cells
		T1: 4 natalizumab infusions	**T1: 4 natalizumab infusions**
Sample type	***n*° + patients**	**JCPyV average value**	**JCPyV average value**
Urine	9	$7{,}5 \times 10^4$ gEq/mL	
Plasma	3	4×10^3 gEq/mL	
Pbmc	2	1×10^3 gEq/10^6 cells	
Plasma + PBMC	1	$9{,}5 \times 10^2$ gEq/mL	3×10^2 gEq/10^6 cells
		T2: 8 natalizumab infusions	**T2: 8 natalizumab infusions**
Sample Type	***n*° + patients**	**JCPyV average value**	**JCPyV average value**
Urine	15	$9{,}5 \times 10^4$ gEq/mL	
Plasma	4	$6{,}5 \times 10^3$ gEq/mL	
PBMC	3	1×10^3 gEq/10^6 cells	
Plasma + PBMC	1	9×10^2 gEq/mL	$3{,}5 \times 10^2$ gEq/10^6 cells
		T3: 12 natalizumab infusions	
Sample type	***n*° + patients**	**JCPyV average value**	
Urine	18	$2{,}5 \times 10^5$ gEq/mL	
Plasma	7	7×10^3 gEq/mL	
PBMC	5	$1{,}5 \times 10^3$ gEq/mL	
		T4: 16 natalizumab infusions	**T4: 16 natalizumab infusions**
Sample type	***n*° + patients**	**JCPyV average value**	**JCPyV average value**
Urine	22	$5{,}5 \times 10^5$ gEq/mL	
Plasma	6	4×10^4 gEq/mL	
PBMC	5	3×10^3 gEq/10^6 cells	
Plasma + PBMC	1	$3{,}5 \times 10^4$ gEq/mL	1×10^2 gEq/10^6 cells
Urine + Plasma	6	$2{,}5 \times 10^5$ gEq/mL	3×10^4 gEq/mL
		T5: natalizumab infusions	**T5: 20 natalizumab infusions**
Sample type	***n*° + patients**	**JCPyV average value**	**JCPyV average value**
Urine	25	$9{,}5 \times 10^5$ gEq/mL	
Plasma	9	$5{,}5 \times 10^4$ gEq/mL	
PBMC	5	4×10^3 gEq/10^6 cells	
Urine + Plasma	6	$6{,}5 \times 10^5$ gEq/mL	$3{,}5 \times 10^4$ gEq/mL

PBMC: peripheral blood mononuclear cells; n°+: number of JCPyV positive patients; gEq/mL: genome equivalents/milliliter; gEq/10^6 cells: genome equivalents/10^6 cells for PBMC.

JCV®-positive patients and 9 among STRATIFY JCV®-negative patients. In particular, the STRATIFY JCV®-positive patient presented viral DNA in plasma and in PBMC, simultaneously (Table 3). By contrast, among 9 STRATIFY JCV®-negative patients, 4 exhibited JC viruria, 3 were viremic and 2 showed a JCPyV DNA in PBMC (Table 3). At T3, the *scenario* changed: the number of STRATIFY JCV®-positive patients increased from 8 to 12, whereas all RRMS patients revealed JCPyV DNA.

Specifically, among 12 STRATIFY JCV®-positive patients, 5 (STRATIFY JCV®-negative and negative for JCPyV viruria at T0) had viruria and 4 viremia (1 already STRATIFY JCV®-positive and viremic at T0 and the remaining 3 featured a new diagnosis of viremia) (Table 3). Finally, 3/12 T3-STRATIFY JCV®-positive patients were positive for JCPyV DNA in PBMC: 1 patient, at T0, was STRATIFY JCV®-positive and positive for JCPyV DNA in PBMC, whereas, the residual 2 patients

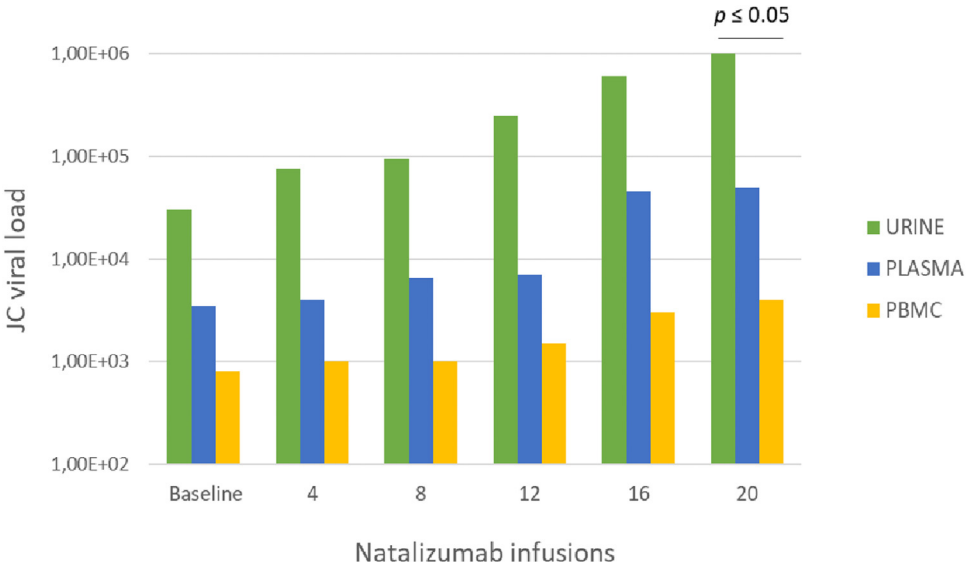

Fig. 2. Statistical analysis of the JC viral load with respect natalizumab infusions in urine, plasma and PBMC during the whole study. The average value of JC viruria was always significantly higher than JC viremia average value. Statistical analysis was performed using nonparametric tests and significance was set for a p value <0.05.

Table 3
Contextual analysis of the anti-JCPyV antibodies versus JCPyV-DNA detection. At T0, JCPyV-specific antibodies were observed in serum of 8 patients whereas 22 showed a negative STRATIFY JCV®. Contextually to the analysis of the anti-JCPyV antibodies, JCPyV-DNA detection showed a positivity in 10/30 RRMS patients: 1 among 8 STRATIFY JCV®-positive patients and 9 among STRATIFY JCV®-negative patients. Only one STRATIFY JCV®-positive patient presented viral DNA in plasma and in PBMC, simultaneously. Among 9 STRATIFY JCV®-negative patients, 4 had JC viruria, 3 were viremic and 2 were in PBMC. At T3 the number of STRATIFY JCV®-positive patients was 12, whereas all RRMS patients revealed JCPyV DNA. Among 12 STRATIFY JCV®-positive patients, 5 had viruria, 4 viremia and 3 were positive in PBMC. In the remaining 18 STRATIFY JCV®-negative patients, 13 resulted JCPyV DNA positive in urine, 3 were positive in plasma and 2 were positive in PBMC.

T0: baseline Patients stratify JCV® +	Patients JCPyV DNA +	Contextual positivity to stratify JCV® and JCPyV DNA	SAMPLE OF JCPyV-DNA DETECTION
8/30	10/30	1/8	Plasma and PBMC (1)
Patients stratify JCV® - 22/30	10/30	9/22	Urine (4), Plasma (3), PBMC (2)
T3: 12 Natalizumab infusions Patients stratify JCV® +	**Patients JCPyV DNA +**	**Contextual positivity to stratify JCV® and JCPyV DNA**	**SAMPLE OF JCPyV-DNA DETECTION**
12/30	30/30	12/12	Urine (5), Plasma (4), PBMC (3)
Patients stratify JCV® - 18/30	30/30	18/18	Urine (13), Plasma (3), PBMC (2)

Patients stratify JCV® +: patients stratify JCV® positive; patients JCPyV DNA +: patients JCPyV DNA positive.;patients stratify JCV® -: patients stratify JCV® negative.

presented a new positivity for JCPyV in PBMC, at T3 (Table 3). Among the remaining 18 STRATIFY JCV®-negative patients, JCPyV-DNA detection provided positive results in all analyzed patients. Specifically, 13 patients resulted JCPyV DNA positive in urine (the number increased from 4 to 13), whereas patients, positive to DNA detection in plasma (3 samples) and in PBMC (2 samples), conserved the same positivity, previously diagnosed at T0 (Table 3).

3.3. NCCR and VP1 sequences' evaluation

At T0, JCPyV NCCR analysis showed a structural organization similar to archetype JCPyV in all RRMS patients' samples (Fig. 3A). During the follow-up less than 12 months, point mutations were identified. In particular, in plasma of a patient T0-T3 STRATIFY JCV®-negative after one year of natalizumab treatment, a nucleotide transition 208A→G was found inside box F, involving NF-1 binding site (Fig. 3B). In plasma and PBMC samples of two different patients T0-T3 STRATIFY JCV®-negative, NCCR sequence showed a 37T→G transversion in box B, inside the binding site for the cellular transcription factor Spi-B (Fig. 3C). Finally, a sequence obtained from plasma and PBMC, belonging to the only patient T0-T3 STRATIFY JCV®-positive, displayed the transition 217G→A in box F (Fig. 3D). Analysis of NCCR of RRMS patients, treated with natalizumab for more than 12 months, showed identical point mutations already observed in plasma and PBMC during the first year of natalizumab infusions, in the same patients. Remarkably, plasma of T0-T3 STRATIFY JCV®-negative patient, that displayed the transversion 37T→G in Spi-B binding site (box B), showed, after 16 natalizumab infusions (T4), an arranged NCCR, characterized by a duplication of NF-1 cellular transcription factor binding site (box F) and by a box D composed only of 10 out of 65 bases (nucleotides from 117 to 126). The resulted NCCR was A– B*–C–(D)–E–F* (Fig. 4A). Analysis of PBMC, belonging to a patient T0-T3 STRATIFY JCV®-negative and with a transversion 37T→G in Spi-B binding site (box B), displayed, after 20 natalizumab infusions (T5), an arranged NCCR with duplication of box C and deletion of nucleotides from 117 to 180, corresponding to box D. This deletion conferred the following NCCR-box organization: A–B*–C–C–E–F (Fig. 4B).

Regarding JCPyV VP1 sequence analysis, results showed that genotypes 1A and 1B were always observed for the whole duration of the study. After 12 months of natalizumab infusions, in two different patients STRATIFY JCV®-negative at T3, the amino acid change mutations S269F in plasma and S267L in PBMC, involving the receptor-binding region of VP1, were observed. In detail, S267L corresponded to 1A genotype whereas S269F was related to 2B genotype.

3.4. Phylogenetic analysis

Phylogenetic analysis, carried out on VP1 sequences, revealed that all isolates were 99% identical to the reference AB081613, suggesting a stability and a similarity across different isolates of JCPyV VP1.

4. Discussion

Since PML is the main restriction to natalizumab administration, it is crucial to stem this limitation by identifying *biomarkers* able to support the established factors for PML risk stratification on single RRMS patients.

To achieve this goal, our study was addressed to assess if JCPyV-DNA detection could play a role of viral reactivation and infection's *biological marker*. Our results showed that JC viral DNA was detected in urine, plasma and PBMC for the whole study, although JC viral load in urine was significantly higher compared to viremia at all selected time points. This result could be explained assuming that, the decrease of immunosurveillance at the urinary level, caused by natalizumab, determines, firstly, a higher JCPyV replication in renal cells with a viral shedding and, as expected from JCPyV biology, a subsequent release of JCPyV–infected cells into bloodstream (Chen et al., 2009). Moreover, reduced immunosurveillance determined an increment in JC viral load, from T0 to T5, which followed a linear trend with natalizumab infusions' number (Pietropaolo et al., 2015). To further corroborate that viral DNA detection could be considered a valid JCPyV *alert*, a contextual analysis of anti-JCPyV antibodies versus JC viral load, was carried out at T0 and at T3. Results of STRATIFY JCV® did not always correlate with Q-PCR data. In fact, at baseline, only 1 patient exhibited anti-JCPyV antibodies and viral DNA in plasma and in PBMC, simultaneously. At T3, although the number of STRATIFY JCV®-positive patients increased to 12, each RRMS patients presented JCPyV DNA, probably ascribed to JCPyV reactivation's occurrence at visit calendar time, when anti-JCPyV antibodies are still absent, despite viral replication, and to a low anti-JCPyV antibody titer, not detectable by STRATIFY JCV® assay (Berger et al., 2013). In fact, although second-generation STRATIFY JCV® showed an increased sensitivity, some patients present a negativity to anti-JCPyV antibodies and a detectable JCPyV DNA in urine or blood. Our data confirm that anti-JCPyV antibodies assay, alone, is not sufficient for JCPyV diagnosis and should be associated with JCPyV-DNA detection in different body compartments, in order to accurately identify JCPyV infected patients (Fragoso et al., 2013; Major et al., 2013; Delbue et al., 2015). Consequently, different approaches to detect JCPyV infection are required for a more accurate

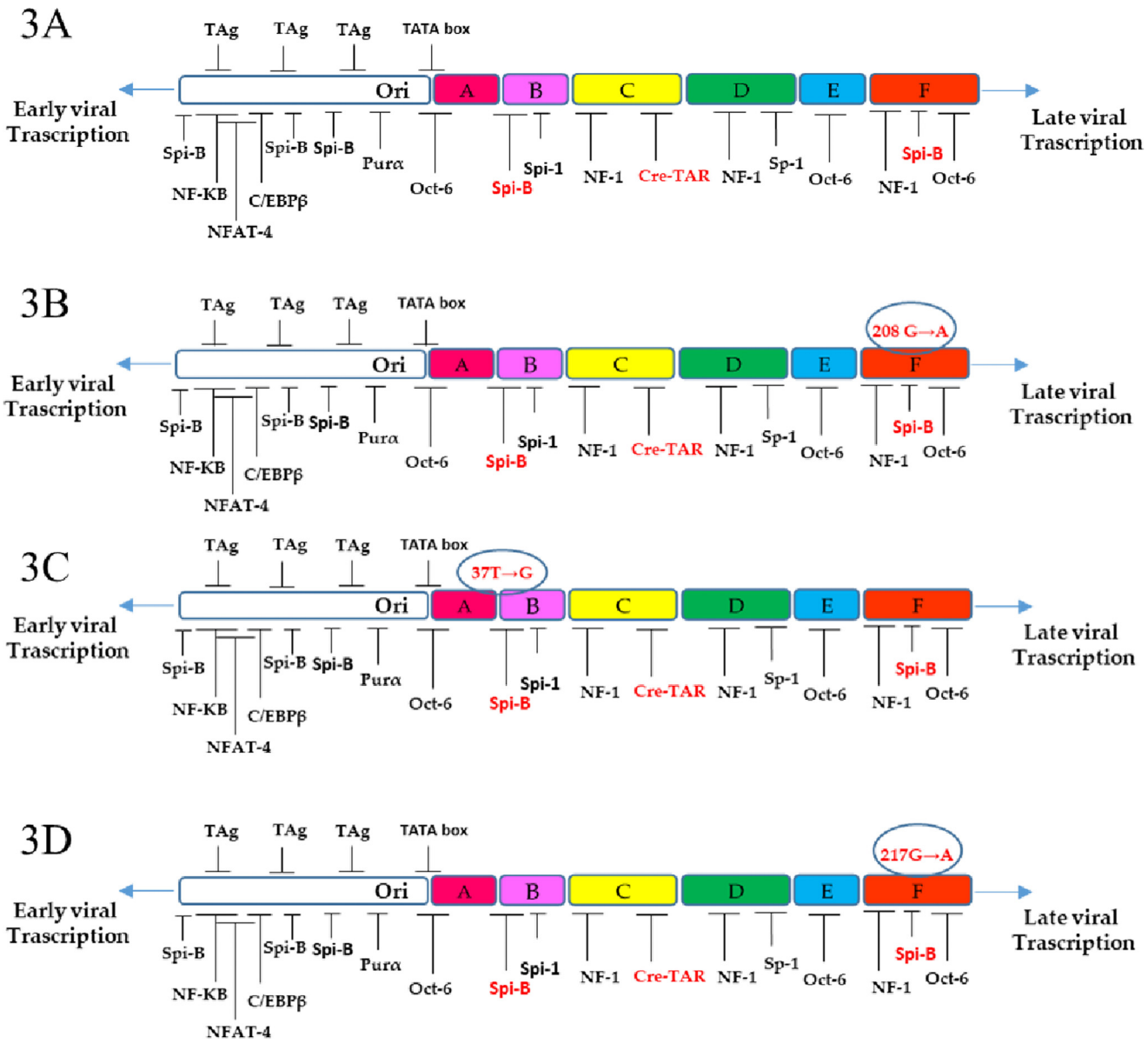

Fig. 3. NCCR analysis during the firt year of natalizumab treatnment (T0–T3). A: an archetype JCPyV NCCR, observed in all RRMS patients' samples at T0, was showed. B: after one year of natalizumab infusions, a nucleotide transition 208A→G was found inside box F (involving NF–1 binding site) in plasma of a patient T0–T3 STRATIFY JCV®-negative. C: NCCR sequence showed a 37T→G transversion in box B (inside Spi-B binding site) in plasma and PBMC samples of two different patients, T0–T3 STRATIFY JCV®-negative. 3D: NCCR obtained from plasma and PBMC, belonging to the only patient T0–T3 STRATIFY JV®-positive, displayed the transition 217G→A in box F.

PML risk monitoring and for the evaluation of those patients, who should start or are already receiving natalizumab. A restriction to JCPyV-DNA detection, as a predictive PML-*biomarker,* could be that JCPyV specific Q-PCR is not able to discriminate between archetype and rr-NCCR. Development of a Q-PCR assay, that specifically identify neurotropic strains, could be an important advance in PML diagnostics (Ryschkewitsch et al., 2013), although it is more difficult, owing to the multitude of arrangements that can occur to yield a more virulent virus. In this framework, since it is possible to speculate that the higher the JC viremia, the higher the possibility that the pathogenic JCPyV emerges, consider Q-PCR data and consequently analyze NCCR sequence could be useful to identify variants correlated with PML. Sequence analysis exhibited an archetype-like structural organization in all analyzed samples during the follow-up less than 12 months, although point mutations, previously observed by other authors in vivo and in vitro (Pietropaolo et al., 2015; Prezioso et al., 2017, 2018), were identified in plasma of 3 T0–T3 STRATIFY JV®-negative patients and in plasma and PBMC of 1 T0-T3 STRATIFY JV®-positive patient.

It is important to remark that the 37T→G transversion in Spi-B binding site of box B, preceded NCCR re-organization and, in particular, it is able to transform archetype Spi-B binding site in a JCPyV PML-variant. This change could enhance JCPyV replication, especially in glial cells, B cells and hematopoietic progenitor cells, in which Spi-B has been shown to be up-regulated (Marshall et al., 2012).

In one plasma's patient, in addition to transversion 37T→G, JCPyV NCCR showed a rearranged structure with duplication, involving NF-1 binding site (box F), and a box D composed of nucleotides from 117 to 126. It is known that NF-1 increased the expression of JCPyV's early and late genes, promoting onset of JCPyV variants with determinants of neurotropism and increased neurovirulence (White et al., 2009). Instead, in PBMC of a patient with 20 natalizumab infusions (T5), in addition to 37T→G mutation, JCPyV-NCCR showed an organization of type A–B*–C–C–E–F, with a duplication of box C, which includes duplication of CRE element binding site, and deletion of box D. The

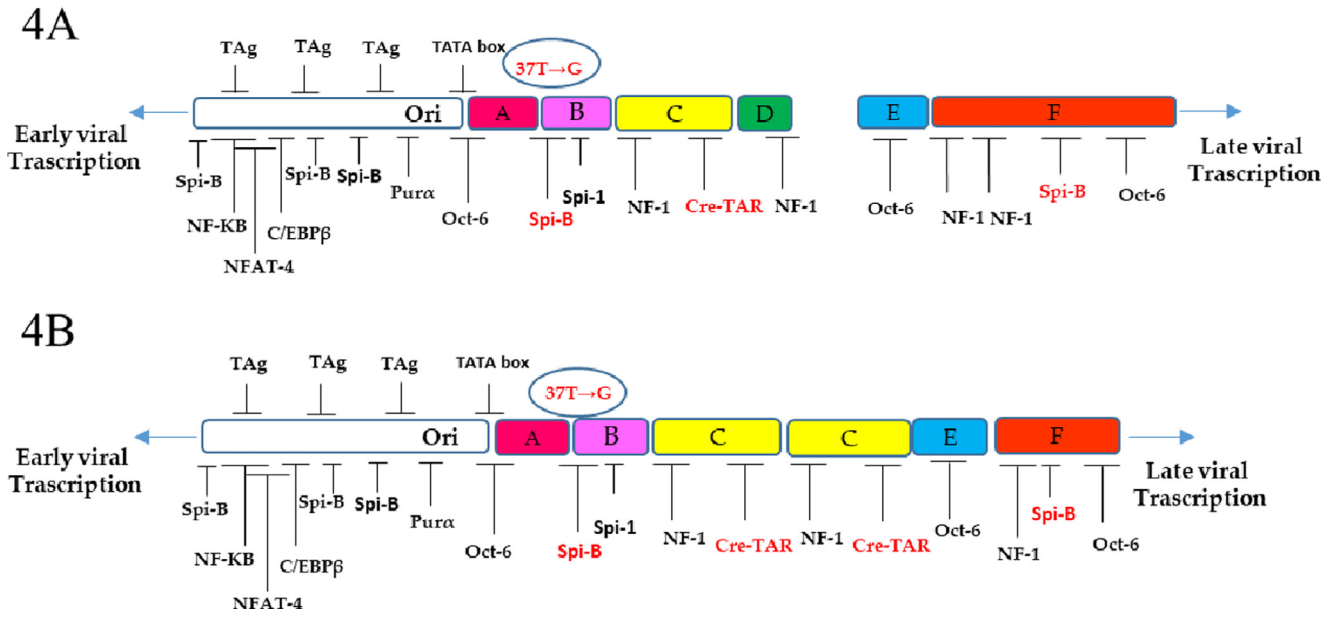

Fig. 4. NCCR analysis after one year of natalizumab treatnment (T4–T5).
A: at T4, plasma of T0–T3 STRATIFY JCV®-negative patient displayed NCCR with the transversion 37T→G in Spi-B binding site (box B), duplication of NF-1 cellular transcription factor binding site (box F) and a box D composed only of 10 out of 65 bases (nucleotides from 117 to 126). The resulted NCCR was A– B*–C–(D)–E–F*. B: at T5, PBMC, belonging to a patient T0-T3 STRATIFY JCV®-negative, showed a transversion 37T→G in Spi-B binding site (box B), duplication of box C and deletion of nucleotides from 117 to 180, corresponding to box D. This deletion conferred the following NCCR-box organization: A–B*–C–C–E–F.

potential neurovirulence of this sequence was conferred by repetition of CRE element, a specific enhancer of JCPyV replication in glial cells in box C (Kumar et al., 1996). NCCR box duplications were recurrently found near to the origin of genome replication (left box A to C), whereas deletions were more frequent near to late genes (right box D to F) (White et al., 2009). Duplications in the left end of NCCR represent a gain of function, increasing activating control sequences that enhance viral replication and gene transcription whereas deletions, in proximity of late genes, determine a loss of function, removing a suppressing control sequence (White et al., 2009).

Regarding VP1 analysis, although this gene is highly polymorphic, only in two different T3 STRATIFY JCV®-negative patients, mutations S269F and S267L were observed in plasma and in PBMC, respectively. Therefore, variations in VP1 region could change the virus's binding properties to its receptor or drive to alternative receptor usage (Sunyaev et al., 2009).

Although JCPyV NCCR arrangements and VP1 mutations are independent events that impact distinct elements of JCPyV cellular tropism, our results highlight to consider NCCR and VP1 modifications as *biomarkers* to monitor the onset of neurovirulent variants.

5. Conclusion

To conclude, we highly recommend considering JCPyV-DNA detection in order to accurately identify JCPyV infected patients with a specific antibodies not yet detectable. Moreover, since a higher JC viremia linked to the possibility that neuro-pathogenic JCPyV emerges, monitoring the trend of JC viral load could be a useful tool to identify mutations and/or NCCR re-organization correlated with neuro-virulent variants. Taking in account these viral *biomarkers* could improve PML risk stratification supporting a timely diagnosis, optimizing health resources and contributing to the reduction of direct and indirect costs of MS disease.

Informed consent

Informed consent was obtained from all individual participants included in the study.

Funding

Anna Teresa Palamara: Funding acquisition (MIUR-PRIN Grant: 2015W729WH); Valeria Pietropaolo: Funding acquisition (MIUR Research Grant: RP118163D5757CA6).

CRediT authorship contribution statement

Carla Prezioso: Conceptualization, Methodology, Data curation, Writing - original draft, Writing - review & editing. **Maria Antonella Zingaropoli:** Conceptualization, Methodology, Writing - review & editing, Data curation. **Marco Iannetta:** Conceptualization, Methodology, Writing - review & editing. **Donatella Maria Rodio:** Conceptualization, Methodology, Writing - review & editing. **Marta Altieri:** Resources, Data curation. **Antonella Conte:** Resources, Data curation. **Vincenzo Vullo:** Writing - review & editing. **Maria Rosa Ciardi:** . **Anna Teresa Palamara:** Funding acquisition, Writing - review & editing. **Valeria Pietropaolo:** Conceptualization, Methodology, Data curation, Writing - original draft, Writing - review & editing, Funding acquisition.

Declaration of Competing Interest

The authors declare that they have no competing interests.

Acknowledgments

Carla Prezioso was supported by funding dispensed by Italian Ministry of Health (starting Grant: SG-2018-12366194).

References

Berger, J.R., 2017. Classifying PML risk with disease modifying therapies. Mult. Scler. Relat. Disord. 12, 59–63. https://doi.org/10.1016/j.msard.2017.01.006.
Berger, J.R., Houff, S.A., Gurwell, J., Vega, N., Miller, C.S., Danaher, R.J., 2013. JC virus antibody status underestimates infection rates. Ann. Neurol 74, 84–90. https://doi.

org/10.1002/ana.23893.
Biogen. TYSABRI® (natalizumab): PML incidence in patients receiving TYSABRI. 2016. https://medinfo.biogen.com/.
Brooks, B.R., Walker, D.L., 1984. Progressive multifocal leukoencephalopathy. Neurol. Clin. 2, 299–313.
Browne, P., Chandraratna, D., Angood, C., Tremlett, H., Baker, C., Taylor, B.V., Thompson, A.J., 2014. Atlas of multiple sclerosis 2013: a growing global problem with widespread inequity. Neurol. 83, 1022–1024. https://doi.org/10.1212/WNL.0000000000000768.
Chen, Y., Bord, E., Tompkins, T., Miller, J., Tan, C.S., Kinkel, R.P., Stein, M.C., Viscidi, R.P., Ngo, L.H., Koralnik, I.J., 2009. Asymptomatic reactivation of JC virus in patients treated with natalizumab. N. Engl. J. Med. 361, 1067–1074 https://www.nejm.org› doi › full › NEJMoa0904267.
Ciotti, M., Prezioso, C., Pietropaolo, V., 2019. An overview on human polyomaviruses biology and related diseases. Future Virol. 14, 487–501. https://doi.org/10.2217/fvl-2019-0050.
Clerico, M., Artusi, C.A., Liberto, A.D., Rolla, S., Bardina, V., Barbero, P., Mercanti, S.F., Durelli, L., 2017. Natalizumab in multiple sclerosis: long-Term management. Int. J. Mol. Sci. 18, E940. https://doi.org/10.3390/ijms18050940.
ClustalW2–Multiple Sequence Alignment: http://www.ebi.ac.uk/Tools/msa/clustalw2/.
Delbue, S., Branchetti, E., Boldorini, R., Vago, L., Zerbi, P., Veggiani, C., Tremolada, S., Ferrante, P., 2008. Presence and expression of JCV early gene large T antigen in the brains of immunocompromised and immunocompetent individuals. J. Med. Virol. 80, 2147–2152. https://doi.org/10.1002/jmv.21313.
Delbue, S., Elia, F., Carloni, C., Pecchenini, V., Franciotta, D., Gastaldi, M., Colombo, E.S., Carluccio, L., Bellizzi, S., Bergamaschi, A., Ferrante, R., 2015. JC virus urinary excretion and seroprevalence in natalizumab-treated multiple sclerosis patients. J. Neurovirol. 21, 645–652.
Flaegstad, T., Sundsfjord, A., Arthur, R.R., Pedersen, M., Traavik, T., Subramani, S., 1991. Amplification and sequencing of the control regions of BK and JC virus from human urine by polymerase chain reaction. Virology 180, 553–560. https://doi.org/10.1016/0042-6822(91)90069-N.
Fragoso, Y.D., Mendes, M.F., Arruda, W.O., Becker, J., Brooks, J.B., Carvalho, Mde.J., Comini-Frota, E.R., Domingues, R.B., Ferreira, M.L., Finkelsztejn, A., Gama, P.D., Gomes, S., Gonçalves, M.V., Kaimen-Maciel, D.R., Morales, Rde.R., Muniz, A., Ruocco, H.H., Salgado, P.R., Albuquerque, L.B., Gama, R.A., Georgeto, S., Lopes, J., Oliveira, C.L., Oliveira, F.T., Safanelli, J., Saldanha, P.C., Satomi, M., 2013. Nearly one-half of Brazilian patients with multiple sclerosis using natalizumab are DNA-JC virus positive. Arq. Neuropsiquiatr. 71, 780–782.
Giovannoni, G., Bermel, R., Phillips, T., Rudick, R., 2018. A brief history of NEDA. Mult. Scler. Relat. Disord. 20, 228–230. https://doi.org/10.1016/j.msard.2017.07.011.
Gorelik, L., Lerner, M., Bixler, S., Crossman, M., Schlain, B., Simon, K., Pace, A., Cheung, A., Chen, L.L., Berman, M., Zein, F., Wilson, E., Yednock, T., Sandrock, A., Goelz, S.E., Subramanyam, M., 2010. Anti-JC virus antibodies: implications for PML risk stratification. Ann. Neurol. 68, 295–303. https://doi.org/10.1002/ana.22128.
Jin, L., Gibson, P.E., Knowles, W.A., Clewley, J.P., 1993. BK virus antigenic variants: sequence analysis within the capsid VP1 epitope. J. Med. Virol. 39, 50–56. https://doi.org/10.1002/jmv.1890390110.
Jobes, D.V., Friedlaender, J.S., Mgone, C.S., Agostini, H.T., Koki, G., Yanagihara, R., Ng, T.C.N., Chima, S.C., Ryschkewitsch, C.F., Stoner, G.L., 2001. New JC virus (JCV) genotypes from papua new guinea and micronesia (type 8 and type 2E) and evolutionary analysis of 32 complete JCV genomes. Arch. Virol. 146, 2097–2113. https://doi.org/10.1007/s007050170023.
Kleinschmidt-DeMasters, B.K., Tyler, K.L., 2005. Progressive multifocal leukoencephalopathy complicating treatment with natalizumab and interferon beta-1a for multiple sclerosis. N. Engl. J. Med. 353, 369–374. https://doi.org/10.1056/nejmoa051782.
Kumar, S., Nei, M., Dudley, J., Tamura, K., 2008. MEGA: a biologist-centric software for evolutionary analysis of DNA and protein sequences. Brief. Bioinform. 9, 299–306. https://doi.org/10.1093/bib/bbn017.
Kumar, K.U., Tang, S.C., Pater, M.M., Pater, A., 1996. Glial and muscle embryonal carcinoma cell-specific independent regulation of expression of human JC virus early promoter by cyclic amp response elements and adjacent nuclear factor 1 binding sites. J. Med. Virol. 49, 199–204.
Kurtzke, J.F., 1983. Rating neurologic impairment in multiple sclerosis: an expanded disability status scale (EDSS). Neurology 33, 1444–1452. https://doi.org/10.1212/WNL.33.11.1444.
Major, E.O., Frohman, E., Douek, D., 2013. JC viremia in natalizumab-treated patients with multiple sclerosis. N. Engl. J. Med. 368, 2240–2241 https://www.nejm.org › 10.1056 › NEJMc1214233.
Major, E.O., Yousry, T.A., Clifford, D.B., 2018. Pathogenesis of progressive multifocal leukoencephalopathy and risks associated with treatments for multiple sclerosis: a decade of lessons learned. Lancet Neurol 17, 467–480. https://doi.org/10.1016/S1474-4422(18)30040-1.
Mancuso, R., Saresella, M., Hernis, A., Marventano, I., Ricci, C., Agostini, S., Rovaris, M., Caputo, D., Clerici, M., 2012. JC virus detection and JC virus-specific immunity in natalizumab-treated multiple sclerosis patients. J. Transl. Med. 10, 248. https://doi.org/10.1186/1479-5876-10-248.
Markowitz, R.B., Thompson, H.C., Mueller, J.F., Cohen, J.A., Dynan, W.S., 1993. Incidence of BK virus and JC virus viruria in human immunodeficiency virus-infected and uninfected subjects. J. Infect. Dis. 167, 13–20. https://doi.org/10.1093/infdis/167.1.13.
Marshall, L.J., Moore, L.D., Mirsky, M.M., Major, E.O., 2012. JC virus promoter/enhancers contain TATA box-associated Spi-B binding sites that support early viral gene expression in primary astrocytes. J. Gen. Virol. 93, 651–661.
Padgett, B.L., Zu Rhein, G.M., Walker, D.L., Echroade, R., Dessel, B., 1971. Cultivation of papova-like virus from human brain with progressive multifocal leukoencephalopathy. Lancet 1, 1257–1260. https://doi.org/10.1016/S0140-6736(71)91777-6.
Pietropaolo, V., Bellizzi, A., Anzivino, E., Iannetta, M., Zingaropoli, M.A., Rodio, D.M., Morreale, M., Pontecorvo, S., Francia, A., Vullo, V., Palamara, A.T., Ciardi, M.R., 2015. Human polyomavirus JC replication and noncoding control region analysis in multiple sclerosis patients under natalizumab treatment. J. Neurovirol. 21, 653–665. https://doi.org/10.1007/s13365-015-0338-y.
Pietropaolo, V., Prezioso, C., Bagnato, F., Antonelli, G., 2018. John Cunningham virus: an overview on biology and disease of the etiological agent of the progressive multifocal leukoencephalopathy. New Microbiol 41, 179–186.
Polman, C.H., O'Connor, P.W., Havrdova, E., Hutchinson, M., Kappos, L., Miller, D.H., Phillips, J.T., Lublin, F.D., Giovannoni, G., Wajgt, A., Toal, M., Lynn, F., Panzara, M.A., Sandrock, A.W., AFFIRM Investigators, 2006. A randomized, placebo-controlled trial of natalizumab for relapsing multiple sclerosis. N. Engl. J, Med 354, 899–910 https://www.nejm.org › NEJM192802231980115.
Prezioso, C., Scribano, D., Bellizzi, A., Anzivino, E., Rodio, D.M., Trancassini, M., Palamara, A.T., Pietropaolo, V., 2017. Efficient propagation of archetype JC polyomavirus in COS-7 cells: evaluation of rearrangements within the NCCR structural organization after transfection. Arch. Virol. 162, 3745–3752.
Prezioso, C., Scribano, D., Rodio, D.M., Ambrosi, C., Trancassini, M., Palamara, A.T., Pietropaolo, V., 2018. COS-7-based model: methodological approach to study John Cunningham virus replication cycle. Virol. J. 15, 29.
Ryschkewitsch, C.F., Jensen, P.N., Major, E.O., 2013. Multiplex qPCR assay for ultra sensitive detection of JCV DNA with simultaneous identification of genotypes that discriminates non-virulent from virulent variants. J. Clin. Virol. 57, 243–248.
Sunyaev, S.R., Lugovskoy, A., Simon, K., Gorelik, L., 2009. Adaptive mutations in the JC virus protein capsid are associated with progressive multifocal leukoencephalopathy (PML). PLoS Genet 5, e1000368. https://doi.org/10.1371/journal.pgen.1000368.
Tintore, M., Vidal-Jordana, A., Sastre-Garriga, J., 2019. Treatment of multiple sclerosis – success from bench to bedside. Nat. Rev. Neurol. 15, 53–58. https://doi.org/10.1038/s41582-018-0082-z.
Van Assche, G., Van Ranst, M., Sciot, R., Dubois, B., Vermeire, S., Noman, M., Verbeeck, J., Geboes, K., Robberecht, W., Rutgeerts, P., 2005. Progressive multifocal leukoencephalopathy after natalizumab therapy for Crohn's disease. N. Engl. J. Med. 353, 362–368. https://doi.org/10.1056/NEJMoa051586.
White, M.K., Safak, M., Khalili, K., 2009. Regulation of gene expression in primate polyomaviruses. J. Virol. 83, 10846–10856.
Wingerchuk, D.M., Weinshenker, B.G., 2016. Disease modifying therapies for relapsing multiple sclerosis. BMJ 354, i3518. https://doi.org/10.1136/bmj.i3518.
Yogo, Y., Kitamura, T., Sugimoto, C., Ueki, T., Aso, Y., Hara, K., 1990. Isolation of a possible archetypal JC virus DNA sequence from nonimmunocompromised individuals. J. Virol. 64, 3139–3143.